ФИЗИКА

УДК 535.33:539.3.075:621.373.8:621.9.048.7:549.6 DOI: https://doi.org/10.54341/20778708_2025_4_65_29
EDN: ZXSJJW

ИССЛЕДОВАНИЕ И ОПТИМИЗАЦИЯ ЛАЗЕРНОГО РАСКАЛЫВАНИЯ КРИСТАЛЛИЧЕСКОГО КВАРЦА С ИСПОЛЬЗОВАНИЕМ ГЕНЕТИЧЕСКОГО АЛГОРИТМА, НЕЙРОСЕТЕВЫХ И НЕЙРО-НЕЧЕТКИХ МОДЕЛЕЙ

Ю.В. Никитюк, Л.Н. Марченко, А.Н. Сердюков

Гомельский государственный университет имени Франциска Скорины

STUDY AND OPTIMIZATION OF LASER CLEAVING OF CRYSTALLINE QUARTZ USING GENETIC ALGORITHM, NEURAL NETWORK AND NEURO-FUZZY MODELS

Yu.V. Nikityuk, L.N. Marchenko, A.N. Serdyukov

Francisk Skorina Gomel State University

Аннотация. Работа посвящена разработке метамодели процесса лазерного раскалывания кристаллического кварца, включающей моделирование и оптимизацию. На основе конечно-элементной модели с использованием языка программирования APDL определены температурные поля и поля термоупругих напряжений, которые формируются в монокристаллической кварцевой пластине в результате последовательного лазерного нагрева и воздействия хладагента для трех различных вариантов: I – анализ среза *ZY* при перемещении лазерного пучка в направлении оси *X*; II – анализ среза *YX* при перемещении лазерного пучка в направлении оси *X*; III – анализ среза *XY* при перемещении лазерного пучка в направлении оси *Z*. С использованием центрального композиционного плана проведен численный эксперимент, в котором в качестве факторов были использованы скорость обработки, геометрические параметры эллиптического лазерного пучка, мощность CO_2-лазера и толщина кварцевой пластины. Согласно плана численного эксперимента выполнены расчеты для 27 комбинаций факторов с определением значений максимальных температур T_1, T_2, T_3 для трех вариантов обработки квадратной кварцевой пластины и трех соответствующих значений максимальных напряжений растяжения S_1, S_2, S_3, действующих перпендикулярно фронту лазерно-индуцированных трещин. Выявлены эффективные архитектуры искусственных нейронных сетей для определения максимальных температур и максимальных термоупругих напряжений в зоне лазерной обработки кристаллического кварца с использованием TensorFlow. Построены нейро-нечеткие модели в системе ANFIS, проведено сравнение нейросетевых и нейро-нечетких моделей. Определены эффективные входные параметры лазерного раскалывания кристаллического кварца на основе оптимизационного генетического алгоритма MOGA.

Ключевые слова: *лазерная резка*; *искусственные нейронные сети*; *искусственная нейронная сеть*, *основанная на нечеткой системе вывода*; *оптимизационный генетический алгоритм MOGA*; *программа ANSYS.*

Для цитирования: *Никитюк*, *Ю.В*. Исследование и оптимизация лазерного раскалывания кристаллического кварца с использованием генетического алгоритма, нейросетевых и нейро-нечетких моделей / Ю.В. Никитюк, Л.Н. Марченко, А.Н. Сердюков // Проблемы физики, математики и техники. – 2025. – № 4 (65). – С. 29–34. – DOI: https://doi.org/10.54341/20778708_2025_4_65_29. – EDN: ZXSJJW

Abstract. The study focuses on developing a metamodel for the laser cleaving process of crystalline quartz, encompassing modeling and optimization. Using a finite element model implemented in the APDL programming language, temperature fields and thermoelastic stress fields were determined. These fields arise in a monocrystalline quartz plate due to sequential laser heating and coolant exposure, analyzed for three distinct variants: I – analysis of the *ZY*-plane cross-section with laser beam movement along the *X*-axis; II – analysis of the *YX*-plane cross-section with laser beam movement along the *X*-axis; III – analysis of the *XY*-plane cross-section with laser beam movement along the *Z*-axis. A central composite design was employed to conduct a numerical experiment, where the factors included processing speed, geometric parameters of the elliptical laser beam, CO_2 laser power, and quartz plate thickness. According to the experimental design, calculations were performed for 27 factor combinations, determining the maximum temperature values (T_1, T_2, T_3) for three processing variants of a square quartz plate, along with three corresponding values of maximum tensile stress (S_1, S_2, S_3) acting perpendicular to the laser-induced crack fronts. The optimal artificial neural network architectures were identified for predicting maximum temperatures and thermoelastic stresses in the laser processing zone of crystalline quartz using TensorFlow. Neuro-fuzzy models were developed in the ANFIS framework, followed by a comparative analysis of neural network and neuro-fuzzy approaches. Furthermore, the most effective input parameters for laser cleaving of crystalline quartz were determined through optimization using the MOGA.

Keywords: *laser cutting*, *Artificial Neural Networks*, *adaptive network-based fuzzy inference system*, *MOGA optimization genetic algorithm*, *ANSYS program.*

For citation: *Nikityuk*, *Yu.V*. Study and optimization of laser cleaving of crystalline quartz using genetic algorithm, neural network and neuro-fuzzy models / Yu.V. Nikityuk, L.N. Marchenko, A.N. Serdyukov // Problems of Physics, Mathematics and Technics. – 2025. – № 4 (65). – P. 29–34. – DOI: https://doi.org/10.54341/20778708_2025_4_65_29. – EDN: ZXSJJW

1 Introduction

The relevance of studying laser cleaving of crystalline quartz stems from increasing demands for precision and quality in processing brittle non-metallic materials within microelectronics and optoelectronics applications. Traditional machining methods face significant limitations, necessitating novel approaches to enhance the efficiency and quality of quartz cutting. Laser cleaving technology offers an effective solution for brittle material processing, based on generating localized thermoelastic stresses through combined laser irradiation and coolant application. The process involves material heating by laser radiation followed by cooling-induced stress generation, which initiates controlled crack propagation. This technology provides three key advantages: high cutting precision, minimal material damage, and superior processing productivity [1].

Finite element modeling (FEM) has become a widely adopted approach for investigating laser cleaving processes in brittle non-metallic materials [2]–[5]. However, FEM implementations demand substantial computational resources, limiting their utility for real-time process analysis and parameter optimization. This constraint has driven growing interest in metamodeling techniques, which enable significant computational cost reduction through simplified yet sufficiently accurate models derived from FEM-generated datasets [6]. Within this paradigm, artificial neural networks (ANNs) and adaptive neuro-fuzzy inference systems (ANFIS) have demonstrated successful applications in studying laser processing of brittle non-metallic materials. Furthermore, genetic algorithms provide an effective methodology for determining optimal laser processing parameters [7]–[16].

This study implements finite element modeling of controlled laser cleaving processes in crystalline quartz. The resulting simulation data was utilized to develop artificial neural network and neuro-fuzzy models, and to determine optimal parameters for laser-induced crack propagation in crystalline quartz through genetic algorithm optimization.

2 Discussion

The proposed metamodel representing the laser cleaving process of crystalline quartz is shown in Figure 2.1.

Let us examine the key structural components of the metamodel.

I. ***Finite Element Modeling.*** The simulation of temperature fields and thermoelastic stresses arising during controlled laser cleaving of crystalline quartz was performed using a quasi-static formulation with application of uncoupled thermoelasticity theory.

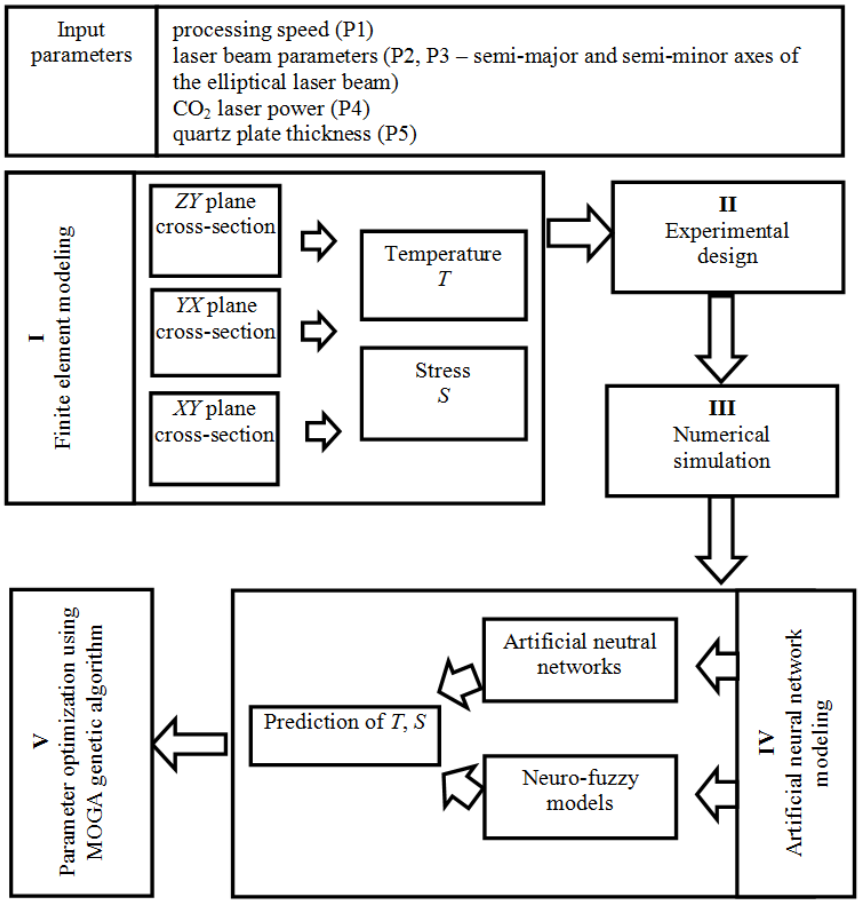

Figure 2.1 – Metamodel of the laser cleaving process for crystalline quartz

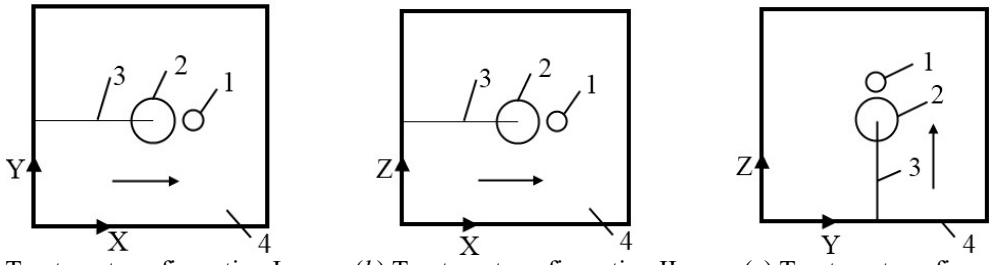

(*a*) Treatment configuration I (*b*) Treatment configuration II (*c*) Treatment configuration III

Figure 2.2 – Layout diagrams of laser irradiation and refrigerant application zones in the processing plane

In the finite element modeling, crystalline quartz was assigned the following material properties: density $\rho = 2643$ kg/m^3 and specific heat capacity $C = 741$ J/(kg·K). The thermal conductivity and linear thermal expansion coefficients were defined as $\lambda_{\parallel} = 12.3$ W/(m·K) and $\alpha_{\parallel} = 9 \cdot 10^{-6}$ K^{-1} along the *Z*-axis (third-order symmetry axis), with perpendicular values $\lambda_{\perp} = 6.8$ W/(m·K) and $\alpha_{\perp} = 14.8 \cdot 10^{-6}$ K^{-1}. The elastic stiffness constants applied in calculations were: $C_{11} = 86.75 \cdot 10^9$ MPa, $C_{12} = 5.95 \cdot 10^9$ MPa, $C_{13} = 11.91 \cdot 10^9$ MPa, $C_{14} = -17.8 \cdot 10^9$ MPa, $C_{33} = 107.2 \cdot 10^9$ MPa, and $C_{44} = 57.8 \cdot 10^9$ MPa [5].

The studies were conducted on square plates measuring 20×20 mm, with sample thickness varying in the range of 0.5 to 2 mm. The modeling was performed for conditions involving laser radiation exposure at a wavelength of 10.6 μm.

The modeling employed standard initial orientations for the square-shaped crystalline samples. For each of the three cross-sections, the laser beam movement direction was aligned with the crystallographic axes lying within the respective processing plane. Notably, following the convention established in [17], the cross-sections were designated using two-letter codes indicating the crystallographic axes: the first letter represents the axis oriented along the sample's thickness direction, while the second denotes the axis aligned with its length.

The thermoelastic field calculations in the monocrystalline quartz plate, resulting from sequential laser heating and coolant application, were performed for three distinct configurations: I – *ZY*-plane analysis with laser beam movement along the *X*-axis, II – *YX*-plane analysis with laser beam movement along the *X*-axis, and III – *XY*-plane analysis with laser beam movement along the *Z*-axis.

Figure 2.2 illustrates the spatial arrangements of laser irradiation and coolant application zones within the processing plane for the three treatment configurations investigated in this study.

The diagram is annotated as follows: (1) laser beam, (2) refrigerant, (3) laser-induced crack, and (4) quartz plate. The horizontal arrow indicates the direction of the sample movement relative to the laser beam and the refrigerant application zone.

II – III. ***Experimental Design and Numerical Simulation.*** A central composite design was implemented in ANSYS DesignXplorer to plan the numerical experiments. The following input parameters were selected: P_1 is the processing speed (V), P_2, P_3 are the semi-major (A) and semi-minor (B) axes of the elliptical laser beam, P_4 is the CO_2 laser power (P), P_5 is the quartz plate thickness (H).

In accordance with the experimental design, simulations were performed for 27 factor combinations. The analysis determined maximum temperature values (T_1, T_2, T_3) for the three processing configurations of square quartz plates described previously, along with the corresponding maximum tensile stress values (S_1, S_2, S_3) acting perpendicular to the laser-induced crack fronts (see Table 2.1).

IV. ***Artificial Neural Network* (*ANN*) *Modeling***. The laser processing simulation using artificial neural networks was implemented with the TensorFlow library. The neural network implementation employed ReLU activation functions and mean squared error (MSE) as the loss metric, with model optimization performed using the Adam optimizer over 300 training epochs. The dataset incorporated the original 27 central composite design configurations supplemented by 100 additional finite element simulation cases, of which 10 were reserved for testing the neural network models (see Table 2.2).

The model quality assessment used the following performance metrics: mean absolute error (*MAE*), root mean square error (*RMSE*), mean absolute percentage error (*MAPE*), and the coefficient of determination (R^2).

The optimal architectures for predicting maximum temperatures were achieved with a [5-50-30-6] neural network for T1 and [5-40-40-6] networks for both T2 and T3. For maximum tensile stress prediction (S1, S2, S3), the best-performing architectures selected through metric analysis were [5-20-30-6], [5-40-40-6], and [5-50-30-6], respectively. The complete evaluation results for all neural network models are provided in Table 2.3.

Subsequently, a neuro-fuzzy model was developed using the ANFIS (Adaptive Neuro-Fuzzy Inference System) framework, i. e., a hybrid architecture integrating neural networks with fuzzy logic principles. The optimization and training of membership functions followed standard artificial neural network algorithms. As detailed in [18], the ANFIS inference system structure comprises five distinct layers.

Table 2.1 – Experimental design and computational results

N	P_1 (V, m/s)	P_2 (A, m)	P_3 (B, m)	P_4 (P, W)	P_5 (H,m)	T_1, °K	T_2, °K	T_3, °K	S_1, MPa	S_2, MPa	S_3, MPa
1	0.015	0.002	0.0015	45	0.00125	780	787	802	66	147	65
2	0.005	0.002	0.0015	45	0.00125	1098	1069	1101	60	141	63
3	0.025	0.002	0.0015	45	0.00125	678	691	698	63	142	61
4	0.015	0.001	0.0015	45	0.00125	914	930	942	55	135	57
5	0.015	0.003	0.0015	45	0.00125	716	712	731	75	156	72
6	0.015	0.002	0.001	45	0.00125	897	904	924	63	143	63
7	0.015	0.002	0.002	45	0.00125	699	706	717	67	150	67
8	0.015	0.002	0.0015	30	0.00125	618	622	632	44	121	48
9	0.015	0.002	0.0015	60	0.00125	942	951	972	88	174	83
10	0.015	0.002	0.0015	45	0.0005	1172	1111	1180	60	65	67
11	0.015	0.002	0.0015	45	0.002	736	738	740	56	129	60
12	0.005	0.001	0.001	30	0.002	1003	1001	1008	38	100	54
13	0.025	0.001	0.001	30	0.0005	875	911	944	35	37	25
14	0.005	0.003	0.001	30	0.0005	1350	1186	1307	114	83	118
15	0.025	0.003	0.001	30	0.002	544	545	546	34	100	39
16	0.005	0.001	0.002	30	0.0005	1272	1219	1200	78	57	83
17	0.025	0.001	0.002	30	0.002	545	546	546	27	94	33
18	0.005	0.003	0.002	30	0.002	618	612	619	47	119	56
19	0.025	0.003	0.002	30	0.0005	623	612	633	56	58	40
20	0.005	0.001	0.001	60	0.0005	2885	2692	2782	163	113	174
21	0.025	0.001	0.001	60	0.002	1210	1211	1211	54	124	65
22	0.005	0.003	0.001	60	0.002	1118	1105	1122	87	166	93
23	0.025	0.003	0.001	60	0.0005	1204	1121	1245	106	107	76
24	0.005	0.001	0.002	60	0.002	1220	1217	1230	67	147	76
25	0.025	0.001	0.002	60	0.0005	968	1037	1045	73	78	53
26	0.005	0.003	0.002	60	0.0005	2184	1935	2057	239	180	248
27	0.025	0.003	0.002	60	0.002	617	619	620	70	143	69

Table 2.2 – Test dataset

N	P_1 (V, m/s)	P_2 (A, m)	P_3 (B, m)	P_4 (P, W)	P_5 (H,m)	T_1, °K	T_2, °K	T_3, °K	S_1, MPa	S_2, MPa	S_3, MPa
1	0.015	0.002	0.0015	45	0.00125	780	787	802	66	147	65
2	0.005	0.002	0.0015	45	0.00125	1098	1069	1101	60	141	63
3	0.025	0.002	0.0015	45	0.00125	678	691	698	63	142	61
4	0.015	0.001	0.0015	45	0.00125	914	930	942	55	135	57
5	0.015	0.003	0.0015	45	0.00125	716	712	731	75	156	72
6	0.015	0.002	0.001	45	0.00125	897	904	924	63	143	63
7	0.015	0.002	0.002	45	0.00125	699	706	717	67	150	67
8	0.015	0.002	0.0015	30	0.00125	618	622	632	44	121	48
9	0.015	0.002	0.0015	60	0.00125	942	951	972	88	174	83
10	0.015	0.002	0.0015	45	0.0005	1172	1111	1180	60	65	67

Table 2.3 – Neural network model evaluation results

Criterion	T_1	T_2	T_3	S_1	S_2	S_3
RMSE	30 K	37 K	31 K	3.8MPa	4.6 MPa	7.0 MPa
MAE	23 K	21 K	19 K	2.7 MPa	5.4 MPa	5.1 MPa
MAPE	2.0%	1.9%	1.7%	3.6%	3.7%	7.3%
R^2	0.9846	0.9799	0.9890	0.9680	0.9849	0.8959

Table 2.4 – Neuro-fuzzy model evaluation results

Criterion	T_1	T_2	T_3	S_1	S_2	S_3
RMSE	66 K	53 K	66 K	9.9 MPa	11.0 MPa	8.3 MPa
MAE	60 K	49 K	60 K	7.9 MPa	9.3 MPa	7.3 MPa
MAPE	7.2%	5.9%	7.0%	11.2%	10.3%	11.3%
R^2	0.9490	0.9601	0.9522	0.7808	0.9222	0.8553

Layer 1 (adaptive) represents fuzzification. This initial adaptive layer handles the conversion of crisp input parameters $x_1, \ldots, x_n$ into fuzzy linguistic variables. The layer outputs are membership function values $\mu_{i,j}$, $i = 1, \ldots k, j = 1, \ldots, n$. Various membership functions (MFs) in this layer generate membership degree assessments from the input variables.

Layer 2 (non-adaptive) represents implication. This layer implements fuzzy "if-then" rules, where each fixed node establishes both the rule content and its position within the fuzzy inference system. The neurons in this layer output firing strengths w_q ($q = 1,\ldots, L$), which quantify the truth values of each rule's premise in the system's knowledge base.

Layer 3 (non-adaptive) represents normalization. This layer performs normalization of rule activation weights (firing strengths). The non-adaptive nodes compute: $\overline{w}_q = \dfrac{w_q}{\sum_{q=1}^{n} w_q}$, where $q = 1, \ldots, L$.

Layer 4 (adaptive) represents defuzzification. This adaptive layer implements the fuzzy inference model, calculating output values $\overline{w}_q f_q$ for each rule's conclusion, where f_q stands for input parameter functions ($q = 1,\ldots, L$).

Layer 5 (non-adaptive) represents output. This final layer computes the system's crisp output value through weighted summation of all incoming signals from Layer 4: $Y = \sum_{q=1}^{L} \overline{w}_q f_q + \overline{w}_0$.

The training process involves simultaneous optimization of both premise parameters and consequent parameters.

A neuro-fuzzy inference system was developed to predict maximum temperatures (T_1, T_2, T_3) and tensile stresses (S_1, S_2, S_3) based on five input parameters: processing speed (V), laser beam elliptical axes (semi-major A and semi-minor B), CO_2 laser power (P), and quartz plate thickness (H). The system implements Sugeno-type if-then rules with linear consequent functions, where crisp input parameters are first converted into fuzzy sets through triangular, trapezoidal, and Gaussian membership functions during the fuzzification stage

If P_1 is A and P_2 is B and P_3 is C and P_4 is D and P_5 is E then Y is out $a_0 + a_1P_1 + a_2P_2 + a_3P_3 + a_4P_4 + a_5P_5$,

where a_0, a_1, …, a_5 signify the coefficients to be determined, and Y denotes either the maximum temperature (T) or maximum tensile stress (S).

The ANFIS neuro-fuzzy model was trained using dataset obtained from numerical experiments. A hybrid learning algorithm combining gradient descent and least-squares estimation was employed, implementing a two-phase optimization process: first, while keeping the premise parameters fixed, it adjusts the consequent parameters using the least-squares method; then, with the consequents held constant, it refines the premise parameters through gradient descent optimization. The training protocol was configured with 10 epochs and a target error tolerance of 0.

Table 2.4 presents the performance metrics of the ANFIS neuro-fuzzy model for predicting both maximum temperatures (T_1, T_2, T_3) and tensile stresses (S_1, S_2, S_3). The developed model demonstrates satisfactory accuracy compared to neural network approaches, while requiring an order of magnitude smaller training dataset than equivalent neural network models.

V. ***Parameter optimization using MOGA genetic algorithm***. The multi-objective genetic algorithm (MOGA) in ANSYS DesignXplorer was implemented to optimize crystalline quartz laser cleaving parameters. This optimization procedure focused specifically on Processing Configuration I. Notably, the developed algorithm provides universal capability for selecting optimal laser processing parameters across all possible crystalline plane orientations.

The optimization considered the following criteria:

$V \rightarrow \max$, $S_1 \rightarrow \max$, $T \leq 1988$ K.

The optimal parameter set was determined for a quartz plate with 0.001 m thickness. The optimized parameters are presented in Table 2.5, with corresponding finite element modeling reference values shown in parentheses. The MOGA algorithm demonstrated high fidelity, with maximum relative error not exceeding 5% across all response predictions.

Table 2.5 – Optimization results

P_1 (V, m/s)	P_2 (A, m)	P_3 (B, m)	P_4 (P, W)	P_5 (H, m)	T_1, °K	S_1, MPa
0.0053	0.0023	0.0017	58	0.001	1381 (1413)	102 (98)

Conclusion

This study has developed an integrated metamodel comprising five key components: finite element modeling (I), experimental design (II) and numerical simulation (III), neural network and neuro-fuzzy system development (IV), genetic algorithm optimization (V) using MOGA methodology.

Using APDL programming language, the finite element model determined temperature distributions and thermoelastic stress fields generated in monocrystalline quartz plates during sequential laser heating and refrigerant application. The numerical investigation analyzed how four key parameters, namely processing speed, elliptical laser beam geometry, CO_2 laser power, and plate thickness, affect peak temperatures and tensile stresses generated during laser cleaving of crystalline quartz, following a central composite design framework for the computational experiment. The study identified optimal artificial neural network architectures for predicting maximum temperatures and stresses under specified input parameters. While ANN models demonstrated high accuracy, the developed ANFIS neuro-fuzzy systems, combining neural networks with fuzzy logic, achieved satisfactory precision with significantly

smaller training datasets. Parameter optimization using the MOGA genetic algorithm in Design-Xplorer yielded effective processing conditions, delivering results with high fidelity (<5% error margin).

The developed metamodel offers an effective practical solution for improving crystalline quartz laser cleaving quality, significantly reducing both time expenditures and computational resource requirements compared to direct numerical simulations or costly physical experiments. Its key advantage lies in genetic algorithm-based process optimization that automatically identifies optimal laser processing parameters (power, speed, beam focus, and plate thickness) to produce clean fracture surfaces with minimal defects. By combining finite element analysis, neural networks, and neuro-fuzzy systems, the model enables rapid high-accuracy process simulation while substantially reducing the need for expensive equipment trial runs on physical equipment.

The proposed metamodel serves as an effective tool for enhancing efficiency, reducing production costs, and ensuring consistent high quality in industrial laser cleaving of quartz.

REFERENCES

1. *Kondratenko*, *V.S*. Precision Cutting of Glass and Other Brittle Materials by Laser-Controlled Thermo-Splitting (Review) / V.S. Kondratenko, S.A. Kudzh // Glass and Ceramics. – 2017. – № 74. – P. 75–81. – https://doi.org/10.1007/s10717-017-9932-1.

2. *Nikityuk*, *Yu.V*. Laser cleaving of brittle nonmetallic materials / Yu.V. Nikityuk, A.A. Sereda, A.N. Serdyukov. – Gomel: Francisk Skorina Gomel State University, 2025. – 217 p.

3. *Kharche*, *Prashant P*. Systematic review of optimization techniques for laser beam machining / Prashant P. Kharche, Vijay H. Patil // Engineering Research Express. – 2024. – Vol. 6, № 2. – DOI: 10.1088/2631-8695/ad594b.

4. *Serdyukov*, *A.N*. Features of controlled laser thermal cleavage of crystalline silicon / A.N. Serdyukov, S.V. Shalupaev, Y.V. Nikityuk // Crystallography Reports. – 2010. – Vol. 55, № 6. – P. 933–937. – DOI: 10.1134/S1063774510060064.

5. *Features of controlled laser thermal cleavage of crystal quartz* / A.N. Serdyukov [et al.] // Crystallography Reports . – 2012. – Vol. 57, № 6. – P. 792–797. – DOI: 10.1134/S1063774512060120.

6. *Jiang*, *P*. Surrogate model-based engineering design and optimization / P. Jiang, Q. Zhou, X. Shao // Springer Singapore: Springer. – 2020. – 240 p. – DOI: https://doi.org/10.1007/978-981-15-0731-1_8.

7. *Kharche*, *P.P*. Systematic review of optimization techniques for laser beam machining / P.P. Kharche, V.H. Patil // Engineering Research Express. – 2024. – Vol. 6 (2). – P. 213–219. – DOI: 10.1088/2631-8695/ad594b.

8. *Nisar*, *S*. Optimization of Laser Beam Geometry for Controlling Thermal Stresses in CO_2 Laser Glass Cutting / S. Nisar // Lasers Manuf. Mater. Process. – 2025. – DOI: 10.1007/s40516-025-00289-6.

9. *Nikityuk*, *Y*. Optimization of two-beam laser cleavage of silicate glass / Y. Nikityuk, A. Serdyukov, I. Aushev // Journal of Optical Technology. – 2022. – Vol. 89, № 2. – P. 121–125.

10. *Parameters optimization of silicate glass two-beam asymmetric laser splitting* / Yu.V. Nikityuk [et al.] // Opticheskii Zhurnal. – 2023. – Vol. 90, № 6. – P. 15–24. – DOI: http://doi.org/10.17586/1023-5086-2023-90-06-15-24.

11. *Nikitjuk*, *Y*. Determination of the Parameters of Controlled Laser Thermal Cleavage of Crystalline Silicon Using Regression and Neural Network Models / Y. Nikitjuk, A. Serdyukov // Crystallography Reports. – 2023. – Vol. 68, № 7. – P. 195–200.

12. *Nikitjuk*, *Y.V*. Determination of the parameters of two-beam laser splitting of silicate glasses using regression and neural network models / Y.V. Nikitjuk, A.N. Serdyukov, I.Y. Aushev // Journal of the Belarusian State University. Physics. – 2022. – № 1. – P. 35–43. – DOI: https://doi.org/10.33581/2520-2243-2022-1-35-43.

13. *Golovko*, *V.A*. Neural network data processing technologies: Textbook / V.A. Golovko, V.V. Krasnoproshin. – Minsk: BSU, 2017. – 263 p

14. *Optimization of Quartz Sol-gel Glass Cutting Parameters by Elliptical Laser Beams Using Neural Network Simulation and Genetic Algorithm* / Y. Nikityuk [et al.] // Recent Advances in Technology Research and Education. Inter-Academia 2023. Lecture Notes in Networks and Systems. – Cham: Springer, 2024. – Vol. 939. – P. 343–350. – DOI: https://doi.org/ 10.1007/ 978-3-031-54450-7_34.

15. *Software Package for Modeling and Optimizing Parameters of Laser Processing of Brittle Non-Metallic Materials Using Laser Splitting Methods* / Y. Nikityuk [et al.] // 2024 8th International Conference on Information, Control, and Communication Technologies (ICCT). Vladikavkaz, Russian Federation. – 2024. – P. 1–3. – DOI: 10.1109/ICCT62929.2024.10874981.

16. *Determining parameters of controlled laser cleaving of silicate glasses using regression, neural network*, *and fuzzy models* / Yu.V. Nikityuk [et al.] // Problems of Physics, Mathematics and Technics. – 2024. – № 2 (59). – P. 32–38.

17. *Glukman*, *L.I*. Piezoelectric quartz resonators / L.I. Glukman. – Moscow: Radio i Svyaz, 1981. – 232 p.

18. *Shtovba*, *S.D*. Designing fuzzy systems using MATLAB tools / S.D. Shtovba. – Moscow: Goryachaya Liniya, 2007. – 284 p.

The article was submitted 08.07.2025.

Информация об авторах

Никитюк Юрий Валерьевич – к.ф.-м.н., доцент
Марченко Лариса Николаевна – к.т.н., доцент
Сердюков Анатолий Николаевич – чл.-корр. НАН Беларуси, д.ф.-м.н., профессор